🔓**Open Access**

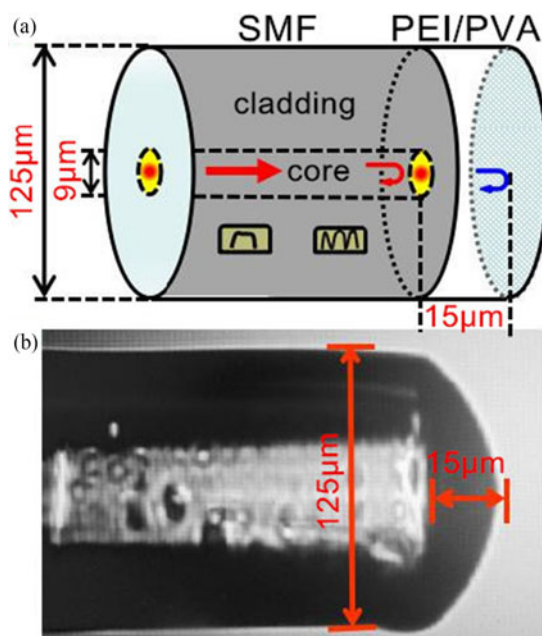# CO_2 Gas Sensing Using Optical Fiber Fabry–Perot Interferometer Based on Polyethyleneimine/Poly(Vinyl Alcohol) Coating

Wenwen Ma
Ruohui Wang
Qiangzhou Rong
Zhihua Shao
Wenlu Zhang
Teng Guo
Jie Wang
Xueguang Qiao

CO$_2$ Gas Sensing Using Optical Fiber Fabry–Perot Interferometer Based on Polyethyleneimine/Poly (Vinyl Alcohol) Coating

Wenwen Ma, Ruohui Wang, Qiangzhou Rong, Zhihua Shao, Wenlu Zhang, Teng Guo, Jie Wang, and Xueguang Qiao

School of Physics, Northwest University, Xi'an 710069, China

Abstract: An optical fiber Fabry–Perot interferometer (FPI) based on poly (ethyleneimine) (PEI)/ poly (vinyl alcohol) (PVA) blend membrane is proposed and realized experimentally as a sensor for the pressure of CO$_2$ in the atmosphere. The functional material layer based on PEI/PVA blend polymer exhibits reversible optical path difference change because of absorption and release of CO$_2$ gas molecules. The cavity of the FPI is fabricated by coating a 15-μm PEI/PVA blend film on the end-face of a cleaved single-mode fiber. An interference spectrum with fringe contrast of 19.5 dB and free spectra range of 33.15 nm is obtained. The proposed FPI sensor is sensitive to the changes of concentration of CO$_2$, as well as a sensitivity of 0.281 nm/% within an interval which ranges from 7.6% to 86.9%.

Index Terms: Thin film coatings, sensors.

1. Introduction

Greenhouse gas emission is believed to be a cause of the global warming and other environmental problems [1]. Carbon dioxide capture and storage (CCS) technology can be used in effectively reducing CO$_2$ emissions [2], [3]. In CCS projects, it is important to accurately monitor the leakage of CO$_2$ at storage area to evaluate the potential risks and hazards to human health [4], [5], and the environment [6]. Currently, optical CO$_2$ sensors mainly include non-dispersive infrared (NDIR) sensor and fluorescence sensor. NDIR spectroscopic sensor detect the absorption band of CO$_2$ at 4.26 um and a high resolution can be achieved, however a bulky optical absorption cell is needed for strong absorption [7], [8]. The operating principle of fluorescence CO$_2$ sensor [9]–[11] is the fluorescent dyes are sensitive to PH change induced by the CO$_2$ absorption. One of the main flaws is the performance of the fluorescence sensor can be degraded by photo bleaching.

Optical fiber sensors are well known for their advantages involving compact size, low cost, high sensitivity and multiplex capability and have been developed for CO$_2$ sensing. Optical fiber CO$_2$ sensors are mainly based on laser absorption spectroscopic method at middle infrared range [12].
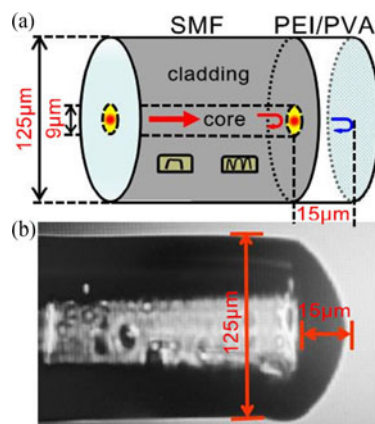
Fig. 1. (a) Schematic diagram of the Fabry–Perot cavity. (b) Microscopic image of the fabricated interferometer.

However, fiber optic components in middle infrared range, such as light source, photo-detector and even optical fiber itself, are very expensive.

The optical Fabry–Perot interferometer (FPI) is a classic sensing component. In previous work, we proposed open-cavity fiber FPIs as a gas-sensor. These sensors are fabricated by splicing capillary tubes or photonic crystal fiber (PCF) with a lead-in single-mode fiber (SMF) [13], [14]. The design of the open channel enables gas to enter or leave the cavity freely, which can be used to measure the refractive index of gas. However, the open cavity FPIs is not able to identify specific gas including CO$_2$. Moreover, the gas concentration change induced refractive index change is too small to be detected. Therefore, the key of using FPI to detect CO$_2$ is to build a Fabry–Perot cavity of which the refractive index is sensitive to CO$_2$ concentration variation.

Transparent CO$_2$ sensitive functional materials can be used to build a FP cavity. The material can react with the carbon dioxide, which will cause refractive index (RI) change of the sensing layer. However, reported CO$_2$ sensors using functional material are generally based on optical fiber refractometers, of which the principle is based on evanescent wave interaction rather than building a cavity with the material itself. For example, SB Hamouda et al. proposed an sensor based on a long period grating (LPG) coated with CO$_2$ sensitive phenol [15]. A CO$_2$ dependent RI change of ∼0.05 RIU is observed in concentration range from 10% to 90%. Therefore, functional film based optical CO$_2$ gas sensors have been proposed. L Melo et al. reported a CO$_2$ gas concentration sensor based a long period grating that was coated with a 365 nm layer of polystyrene and obtained a sensitivity of 1.23 pm/% [16]. G Mi et al. proposed a silicon photonic refractometric CO$_2$ gas sensor employing a micro ring (d = 20 μm) that was coated with 240 nm guanidine polymer and the sensors sensitivity is 0.00354 pm/ppm (0.0354 nm/%) [17]. The proposed sensor in this paper has a better performance in the aspect of sensitivity.

In this paper, we propose a FPI with a CO$_2$ sensitive cavity. The cavity of the FPI is poly(ethyleneimine) (PEI)/ poly(vinyl alcohol) (PVA) blend film coated on the end-face of a SMF. The proposed sensor has advantages of compact size, low cost, simple fabrication and fast response. A sensitivity of 0.281 nm/% in a concentration range of 7.6%–86.9% is obtained, which makes it a good candidate for CO$_2$ leakage monitoring.

2. Fabrication and Principle of Sensor

Fig. 1 shows the schematic diagram and microscopic image of a fabricated FPI. When light is coupled into the FPI, the SMF/blend film interface (facet 1) will reflect a portion of the light because of the Fresnel reflection. The remaining light will propagate into the PEI/PVA blend film, and then is partially reflected by the blend film/air interface (facet 2). Due to the phase difference, the two light beams will interfere with each other.

PEI is a colorless or light yellow viscous liquid. It contains a large number of amines, which can be classified into primary, secondary and tertiary groups. At room temperature and atmospheric pressure, the primary and secondary amino groups can reversibly react with CO$_2$ which yields carbamides. Tertiary amines act as a base in the reaction of CO$_2$ with water. However, PEI liquid is unstable and cannot be directly coated on a fiber end face. PVA is a polymer material with good film-forming property, which can be used as a crosslinking agent. Hence, PEI and PVA are mixed in a certain proportion to form a thin film. In the membrane, PEI serves as a carrier molecule for reacting with CO$_2$ and PVA as a base material for the forming the film. Moreover it has also been found that the transportation of CO$_2$ in the ultra-thin PEI/PVA film is much easier [18], [19].

The process of coating a PEI/PVA blend membrane on the tip of the SMF is similar to that described in our previous work [20]. PEI/PVA blend membrane is prepared by solution casting. 10%(wt/wt) PVA colloidal solution is made by mixing the PVA granules with deionized water. Then the solution is heated at 90 °C for 3 hours to insure the PVA granules are completely dissolved. Next, the PVA colloidal solution is blended with the 98% PEI solution (GBK-PEI3000, Gobekie) of which the molecular weight is 3000 at the volume ratio of 1:1. A stepper motor is used to automatically dip a SMF stub into the PEI/PVA blend solution. After maintaining the fiber ending in the solution for 10 min, the SMF is slowly and vertically pulled out. In order to accelerate the speed of water evaporation and make the PEI/PVA blend adhere firmly onto the fiber ending, the sample is heated in the vacuum oven at a constant temperature of 50 °C for 30 minutes.

PEI/PVA blend membrane is a kind of dense polymer film, which contains a large number of amino groups. According to the Hard Soft Acid Base (HSAB) rule [21], [22], the dense polymer membrane can interact with CO$_2$ molecules at room temperature and normal atmospheric pressure by the amino groups which exist in the backbone of polymer. The interaction is an acid-base equilibrium, which is reversible and leads to the formation of amino formic acid ester and alkyl carbonate. The interaction can be expressed as

$$CO_2 + 2RNH_2 \Longleftrightarrow RNHCOO^- + RNH_3^+ \qquad (1)$$

$$CO_2 + 2R_2NH \Longleftrightarrow R_2NCOO^- + R_2NH_2^+. \qquad (2)$$
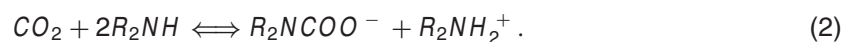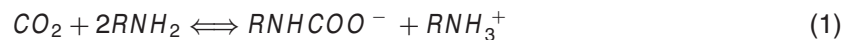
PEI/PVA hybrid film can facilitate the transport of CO$_2$ because there are numerous gas channels on the outer surface. When the concentration of CO$_2$ in the environment is different from that in the membrane, CO$_2$ molecules will diffuse from high concentration to low concentration through the channel of the membrane surface. The system behaves as a dynamic balance. When the PEI/PVA blend film is subjected to a CO$_2$ changing environment, the optical path difference (OPD) of the FPI can be changed. Therefore, CO$_2$ gas concentration can be measured by wavelength shift of interference fringe pattern.

3. Experiment and Discussion

The schematic diagram of the setup for CO$_2$ gas measurement is shown in Fig. 2 . The system consists of a home-made gas chamber and a 2–channel gas controller. The N$_2$ and CO$_2$ gas pass through channels with tunable flow rate up to 2000 sccm and 500 sccm, respectively. Various CO$_2$ concentrations are obtained by changing the flow rate ratio between CO$_2$ and N$_2$ gas. Mixed gas is injected into a home–made gas chamber connected with atmosphere to ensure normal atmospheric pressure. A swept laser based optical spectrum analyzer (OSA, Micron Optics, Inc.; SM 125–700) with a resolution of 5 pm is employed to record the reflective spectrum.

The thickness of the sol-gel film follows the Landau-Levich relationship [23]. According to Landau-Levich relationship, the thickness of the film can be controlled by changing the pulling speed and the concentration of the sol-gel. In our experiment, considering the form of the film and the humidity crosstalk, the volume ratio of PEI/PVA is optimized to be 1:1(V/V). Therefore, the length of the cavity can be controlled only by the pulling speed. Fig. 3(a) presents spectra of FPIs with different cavity length which are fabricated by controlling the pulling speed. Fig. 3(b) shows a typical interference fringe of the PEI/PVA FPI. The thickness of PEI/PVA blend membrane is ∼15 μm.
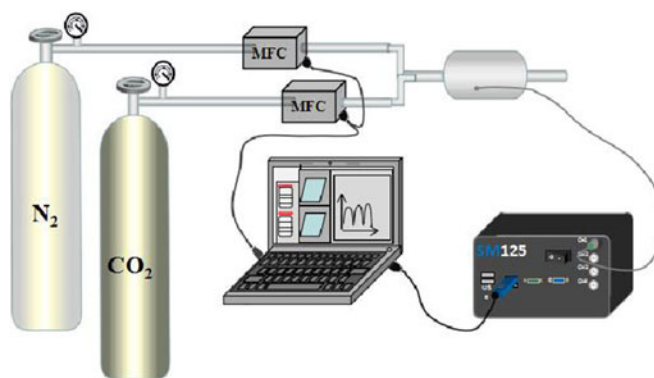
Fig. 2. Schematic diagram of experiment setup for CO$_2$ gas concentration sensing (MFC=mass flow controller).
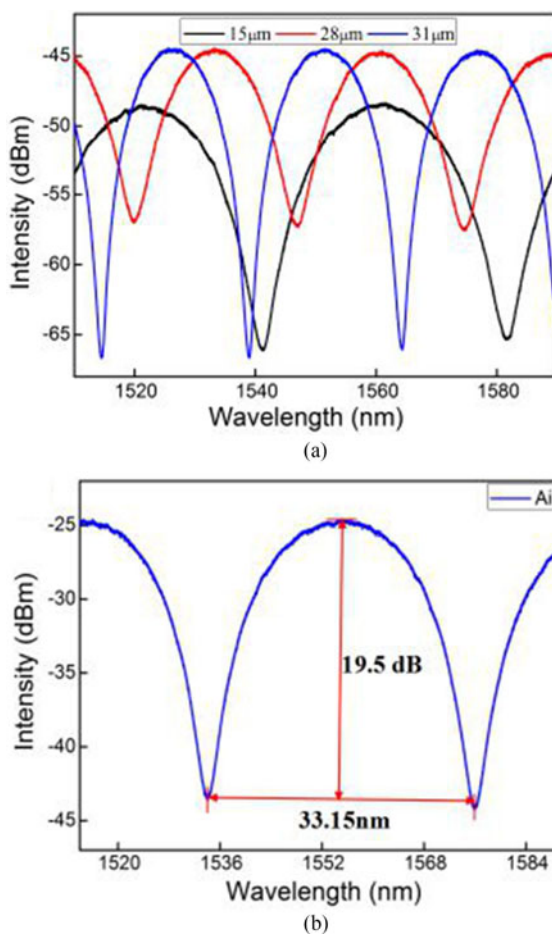

Fig. 3. (a) Reflection spectra of the FPI with different cavity length in the air. (b) Interference spectrum of the L = 15 μm.

The fringe contrast and the free spectral range (FSR) of the FPI are 19.5 dB and 33.15 nm, respectively. Before CO$_2$ concentration measurement, we flush the gas chamber with N$_2$ gas for 5 minutes. The wavelength of the fringe dip at 1527.92 nm gas is selected as the tracing wavelength. By controlling the pump gas flow rate, various concentrations of CO$_2$ gas are flowed through the chamber. In Fig. 4 (a), it can be seen that the tracing wavelength shifts to longer wavelength with
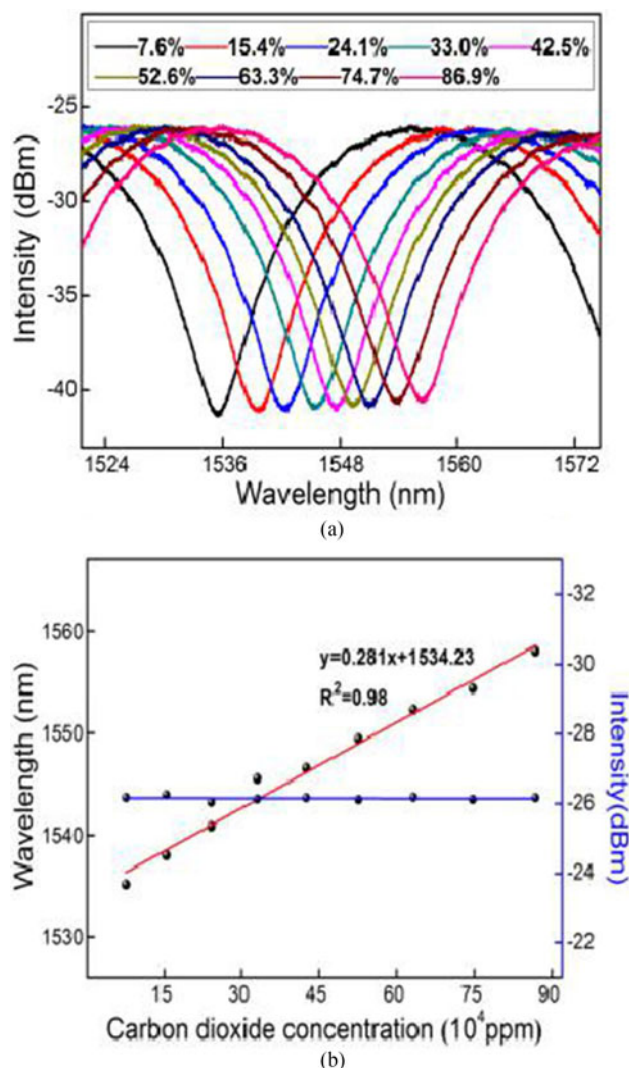
Fig. 4. (a) Wavelength shift with the increasing concentration of CO_2. (b) Linear fitting result of wavelength and energy change as a function of the CO_2 concentration.

the increase of the concentration of CO_2. No obvious intensity change is observed. With a CO_2 concentration change from 7.6% to 86.9%, the total wavelength shift of the selected dip is 22.89 nm and the corresponding RI change of PEI/PVA functional film is 0.0509. As the linear fitting result shown in Fig. 4(b), a CO_2 gas sensitivity of 0.281 nm/% isobtained.

Fig. 5 (a) shows the tracing wavelength shift in a time circle, in which the CO_2 gas concentration increases from 0% to 15.40% and then decreases to 0%. With the increasing of the gas concentration (zone 1), the interference fringe shifts to longer wavelength. After ∼30 s, the spectrum reaches to an equilibration state (zone 2). When purging the chamber with N_2 gas, the fringe shifts back because CO_2 is released from the PEI/PVA blend layer (zone 3). Fig. 5(b) shows the wavelength shift in a more complex time circle. When the concentration of CO_2 in the chamber is increased to 42.5% (zone 1), the PEI/PVA blend membrane reached to an equilibration state (zone 2). The state can be changed by continually increasing the CO_2 concentration of chamber to 100% (zone 1′ and zone 2′). PEI/PVA blend film still can be recovered in a pure N_2 environment (zone 3). The results indicate that the PEI/PVA film has a good recovery capability.
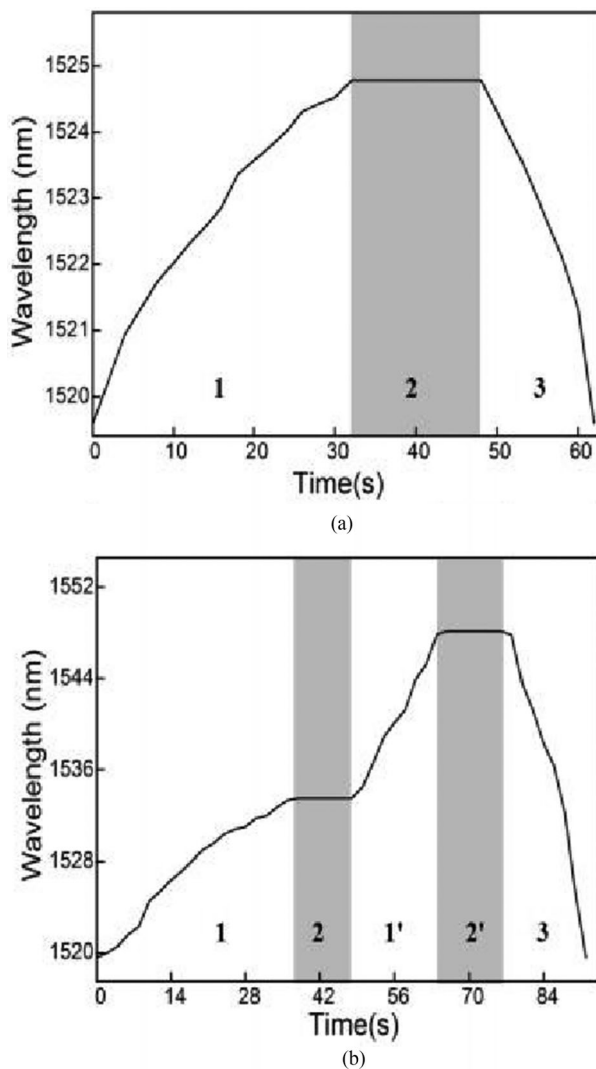
Fig. 5. Wavelength shifts in a CO$_2$ gas concentration variation time circle. (a) 0%–15.4%–0% (b) 0%–42.5%–100%–0%. Zone 1 / 1$'$, zone 2 / 2$'$, and zone 3 represent the states of carbon dioxide absorption, equilibration, and recovery, respectively.

Repeatability is also an important feature to evalate the sensor$'$s performance. Fig. 6 shows the repeatability test of the PEI/PVA blend membrane based optical fiber FPI. In the experiment, the CO$_2$ measurment is repeated for three rounds. From Fig. 6, it can be seen that there is a negligible drift in the base line shift upon repeated exposure of the sensor to the same concentration of CO$_2$. The result demonstrates that such an PEI/PVA FPI also has a good gas concentration RI reproducibility. Due to the properties of the PEI/PVA film, the proposed sensor has a cross-sensitive of temperature and humidity. In practical applications, the sensor needs temperature and humidity compensation. Here, we propose a further solution which is as follows: First, we need to characterize temperature and humidity response of the CO$_2$ sensor independently. Specifically, the temperature response of the sensor are recorded when CO$_2$ concentration and humidity in gas chamber keep constant. Similarly, the humidity response of sensor at a constant CO$_2$ concentration and temperature are obtained. In real applications, a CO$_2$ non-sensitive optical fiber sensor is used to measure the real time temperature and humidity variations of the environment. The sensor for compensation is based on a hybrid structure with a fiber Bragg grating and PVA Fabry-Perot interferometer [20]. With
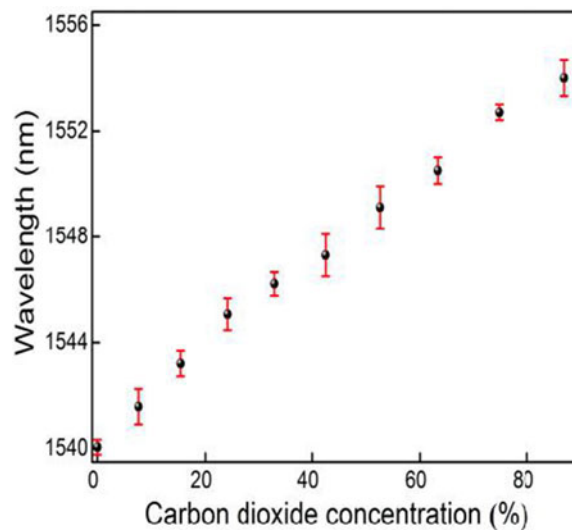
Fig. 6. Repeatability test of the sensor.

information of the real time temperature and humidity, the CO$_2$ concentration measurement results of the proposed sensor can be calibrated according to its response characteristic of temperature and humidity.

4. Conclusion

In this paper, an optical fiber FPI based on PEI/PVA blend membrane is proposed and experimentally demonstrated for CO$_2$ sensing. The PEI/PVA blend film with a thickness of ∼15 μm is coated on the end face of the single-mode optical fiber to form a FP cavity. The proposed sensor is applied in CO$_2$ gas concentration detection and a sensitivity of 0.281 nm/% in 7.6%–86.9% range is obtained. Furthermore, the structure has remote sensing capability as a reflection probe, and since the fabrication is simple and effective, it makes a good candidate for monitoring the leakage of the geological storage of CO$_2$. Compared with commercial CO$_2$ sensors based Quartz Crystal Microbalance (QCM) devices and Surface Acoustic Wave (SAW) devices, the proposed sensor have advantages including small volume, anti-electromagnetic interference and multiplex capability. However, due to the limited resolution of the wavelength tracing demodulation method, the detection limit of the proposed fiber-optic sensor still needs much improvement.

References

[1] M. Meinshausen   et al., "Greenhouse-gas emission targets for limiting global warming to 2 C," *Nature*, vol. 458, no. 7242, pp. 1158–1162, 2009.
[2] L. H. Spangler   et al., "A shallow subsurface controlled release facility in Bozeman, Montana, USA, for testing near surface CO$_2$ detection techniques and transport models," *Environ. Earth Sci.*, vol. 60, no. 2, pp. 227–239, 2010.
[3] K. Romanak, G. W. Sherk, S. Hovorka, and C. Yang, "Assessment of alleged CO$_2$ leakage at the Kerr farm using a simple process-based soil gas technique: Implications for carbon capture, utilization, and storage (CCUS) monitoring," *Energy Procedia*, vol. 37, no. 1, pp. 4242–4248, 2013.
[4] E. R. Siirila, A. K. Navarre-Sitchler, R. M. Maxwell, and J. E. McCray, "A quantitative methodology to assess the risks to human health from CO$_2$ leakage into groundwater," *Adv. Water Resources*, vol. 36, pp. 146–164, 2012.
[5] C. Halsband and H. Kurihara, "Potential acidification impacts on zooplankton in CCS leakage scenarios," *Marine Pollution Bull.*, vol. 73, no. 2, pp. 495–503, 2013.
[6] C. Ma, B. Scott, G. Pickrell, and A. Wang, "Porous capillary tubing waveguide for multigas sensing," *Opt. Lett.*, vol. 35, no. 3, pp. 315–317, 2010.
[7] M. G. Allen   et al., "Ultrasensitive dual-beam absorption and gain spectroscopy: Applications for near-infrared and visible diode laser sensors," *Appl. Opt.*, vol. 34, no. 18, pp. 3240–3249, 1995.

[8]   R. P. Lippmann, "Pattern classification using neural networks," *IEEE Commun. Mag.*, vol. 27, no. 11, pp. 59–64, Nov. 1989.

[9]   R. Selm *et al.*, "Ultrabroadband background-free coherent anti-Stokes Raman scattering microscopy based on a compact Er:fiber laser system," *Opt. Lett.*, vol. 35, no. 19, pp. 3282–3284, 2010.

[10]   M. H. Spalding, C. Critchley, Govindjee, and W. L. Orgren, "Influence of carbon dioxide concentration during growth on fluorescence induction characteristics of the Green Alga Chlamydomonas reinhardii," *Photosynthesis Res.*, vol. 5, no. 2, pp. 169–176, 1984.

[11]   O. S. Wolfbeis, L. J. Weis, M. J. P. Leiner, and W. Z. Ziegler, "Fiber-optic fluorosensor for oxygen and carbon dioxide," *Analytical Chem.*, vol. 60, no. 19, pp. 2028–2030, 1988.

[12]   A. Fomin, T. Zavlev, I. Rahinov, and S. Cheskis, "A fiber laser intracavity absorption spectroscopy (FLICAS) sensor for simultaneous measurement of CO and CO$_2$, concentrations and temperature," *Sensors Actuators B Chem.*, vol. 210, pp. 431–438, 2015.

[13]   R. Wang and X. Qiao, "Hybrid optical fiber Fabry–Perot interferometer for simultaneous measurement of gas refractive index and temperature," *Appl. Opt.*, vol. 53, no. 32, pp. 7724–8, 2014.

[14]   R. Wang and X. Qiao, "Gas refractometer based on optical fiber extrinsic Fabry–Perot interferometer with open cavity," *IEEE Photonics Technol. Lett.*, vol. 27, no. 3, pp. 245–248, Feb. 2015.

[15]   C. Gouveia, A. Markovics, and J. M. Baptista, "Measurement of CO$_2$ using refractometric fiber optic sensors," in *Proc. 3rd WSEAS Int. Conf. Adv. Sensors*, Signals Mater., 2010, pp. 169–173.

[16]   L. Melo, G. Burton, and B. Davies, "Highly sensitive coated long period grating sensor for CO$_2$, detection at atmospheric pressure," *Sensors Actuators B Chem.*, vol. 202, no. 10, 2014, pp. 294–300.

[17]   G. Mi, C. Horvath, and M. Aktary, "Silicon microring refractometric sensor for atmospheric CO$_2$ gas monitoring," *Opt. Exp.*, vol. 24, no. 2, pp. 154–163, 2016.

[18]   L. Deng, T. J. Kim, and M. B. Hagg, "Facilitated transport of CO$_2$, in novel PVAm/PVA blend membrane," *J. Membrane Sci.*, vol. 340, nos. 1/2, pp. 154–163, 2009.

[19]   S. B. Hamouda, Q. T. Nguyen, D. Langevin, and S. Roudesli, "Poly(vinyl alcohol)/poly(ethyleneglycol)/poly(ethyleneimine) blend membranes—Structure and CO$_2$, facilitated transport," *Comptes Rendus Chimie*, vol. 13, no. 3, pp. 372–379, 2010.

[20]   D. Su *et al.*, "A fiber Fabry–Perot interferometer based on a PVA coating for humidity measurement," *Opt. Commun.*, vol. 311, no. 2, pp. 107–110, 2013.

[21]   B. N. Shivananju *et al.*, "CO$_2$ sensing at room temperature using carbon nanotubes coated core fiber Bragg grating," *Rev. of Scientific Instrum.*, vol. 84, no. 6, pp. 065002–065007, 2013.

[22]   T. C. D. Doan, J. Baggerman, R. Ramaneti, H. D. Tong, A. T. M. Marcelis, and C. J. M. van Rijn, "Carbon dioxide detection with polyethylenimine blended with polyelectrolytes," *Sensors Actuators B Chemical*, vol. 201, no. 4, pp. 452–459, 2014.

[23]   C. J. Brinker and G. W. Scherer, *Sol-Gel Science*. New York, NY, USA: Academic, 1990.